QCD Fit Analysis of the Combined H1 and ZEUS Measurement of the Inclusive $e^{\pm}p$ Scattering Cross Sections at HERA including Reduced Proton Beam Energy Runs

H1 and ZEUS Collaborations

Abstract

A QCD fit analysis to the combined HERA-I inclusive deep inelastic cross sections measured by the H1 and ZEUS collaborations for $e^{\pm}p$ scattering including the HERA II measurements with reduced proton-beam energies, $E_p = 460\,\text{GeV}$ and $E_p = 575\,\text{GeV}$, is presented. The effect of including the new data on the determination of HERA parton distribution functions is analysed, using fits similar to those performed for HERAPDF1.0. Some tension of the QCD fit with respect to the data is identified in the kinematic region of low Q^2 and low x. Furthermore, the data show sensitivity to various schemes of treating heavy flavours.
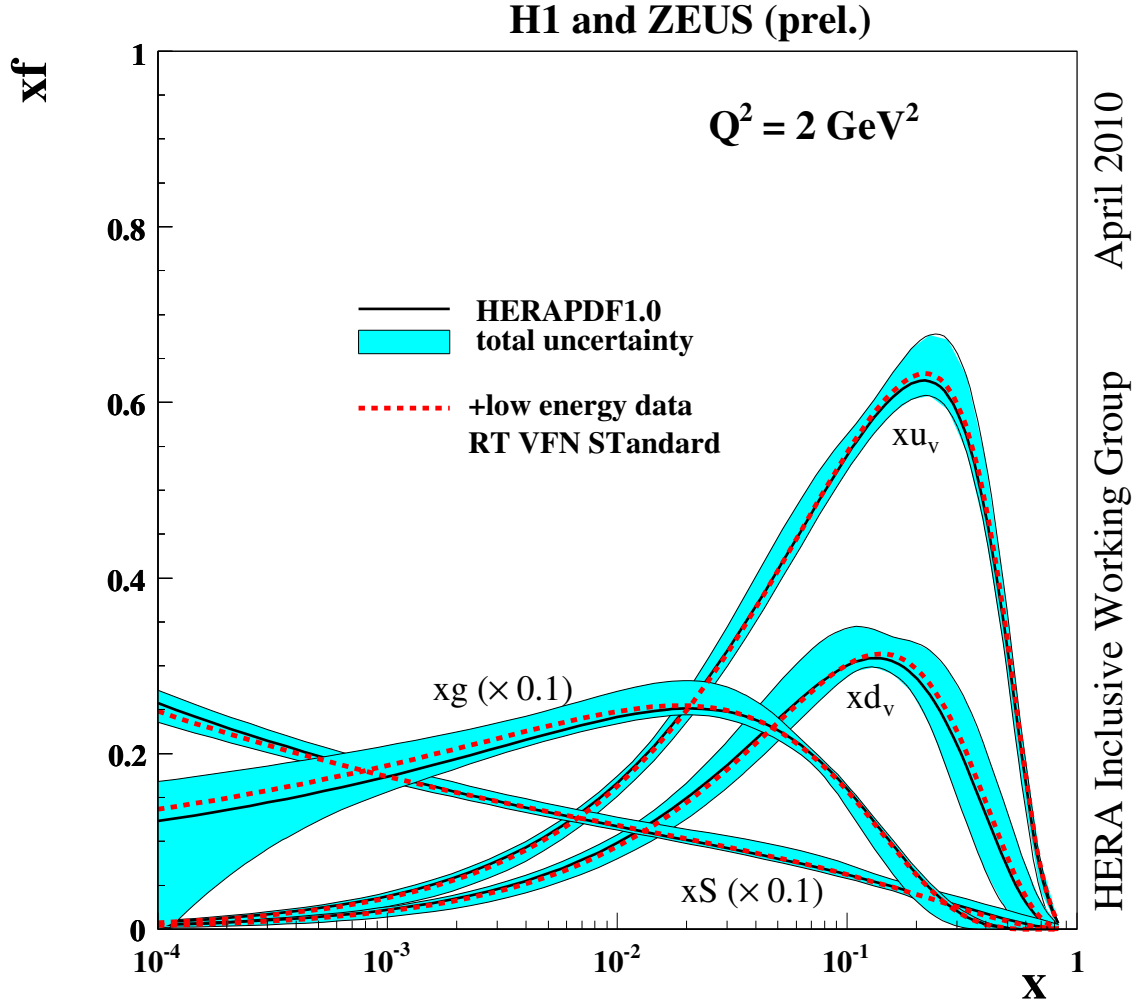
Figure 1: Figure shows a summary of the NLO PDF distributions at the starting scale $Q_0^2 = 1.9$ GeV^2, where HERAPDF1.0 (solid line) with its total uncertainties (blue band) is compared to HERA PDF fit including the reduced proton-beam energy data (doted red line). PDFs shown are valence distributions for up, down, and distributions for the total sea and gluon. Using the same settings as for HERAPDF1.0 (in Roberts and Thorne Variable Flavour Number of Scheme (RTVFNS)), the effect of including the new data is to slightly enhance the gluon distribution. At this scale gluon distribution has a valence-like shape.

	HERAPDF1.0	Including Reduced Proton-Beam Eneregy Data
Total χ^2/dof	574/582	818/806

Table 1: Comparison of the goodness of the fit between HERAPDF1.0 and adding the low energy data. The inclusion of the new data is not fit as well as it could be.
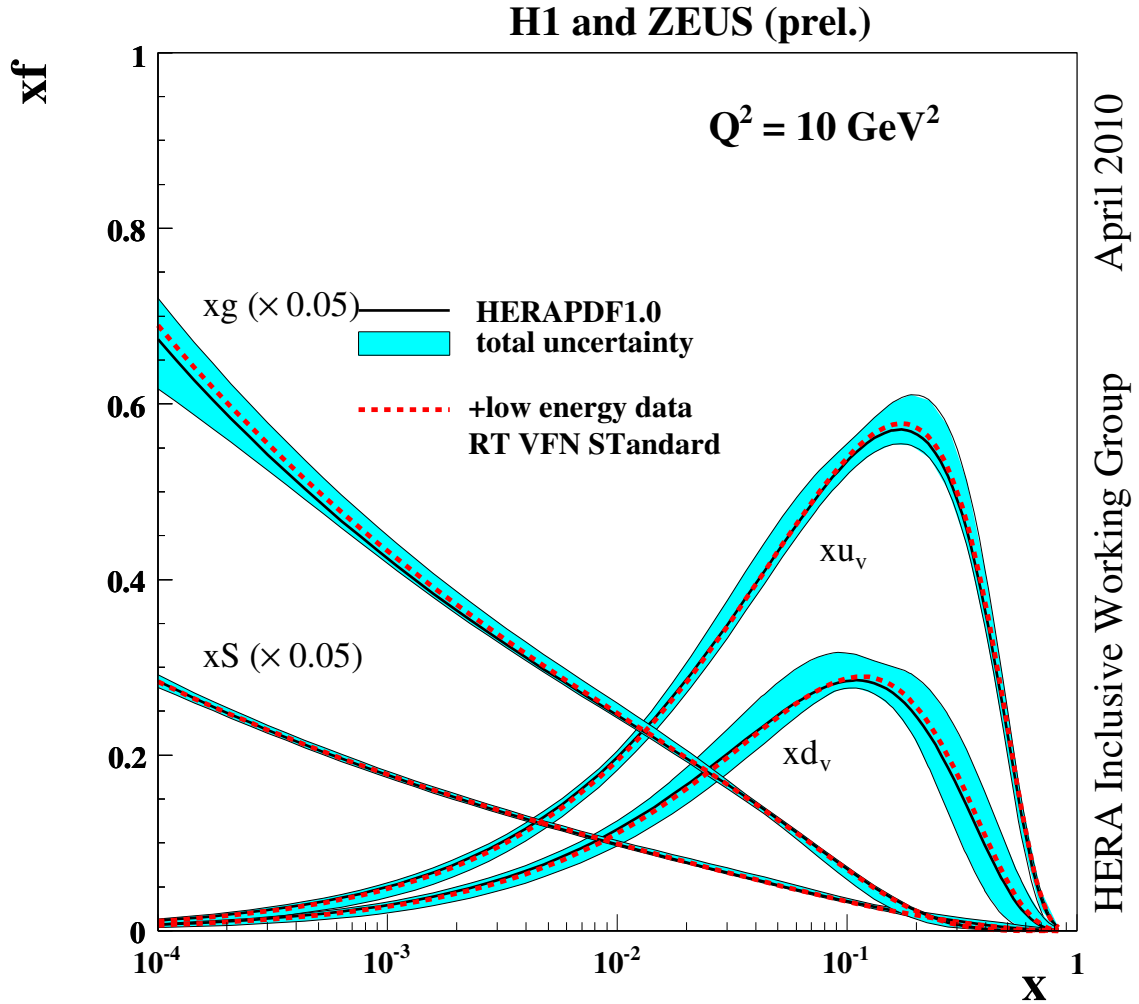
Figure 2: Summary of the NLO PDF distributions at the starting scale $Q_0^2 = 10$ GeV^2, where HERAPDF1.0 (solid line) with its total uncertainties (blue band) is compared to HERA PDF fit including the reduced proton-beam energy data (doted red line). PDFs shown are valence distributions for up, down, and distributions for the total sea and gluon. Using the same settings as for HERAPDF1.0 (in Roberts and Thorne Variable Flavour Number Scheme (RTVFNS)), the effect of including the new data is to slightly enhance the gluon distribution.
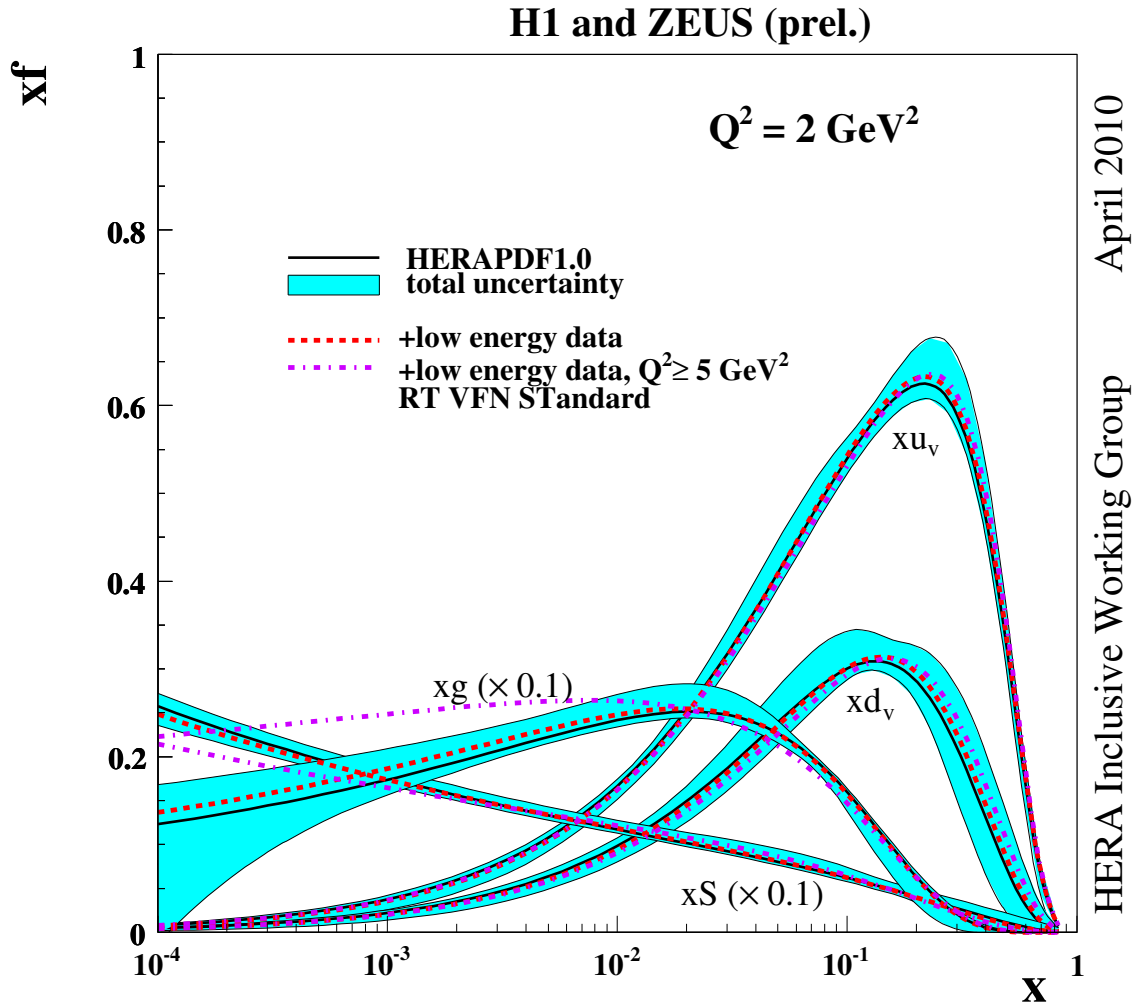
Figure 3: Figure shows summary NLO PDF distributions at the starting scale $Q_0^2 = 1.9$ GeV^2 comparing HERAPDF1.0 (solid line) with its total PDF uncertainties (blue band) to HERA PDF fit with reduced proton-beam energy data using standard settings of HERAPDF1.0 (doted red line) and to new fits using $Q^2 > 5$ GeV^2 cut (dashed magenta line). PDF shown are valence distributions for up, down, and distributions for the total sea and gluon. The kinematic cut $Q^2 > 5$ GeV^2 results in a different PDF solution (best visible on the gluon distribution, where the new fit lies outside of the HERAPDF1.0 uncertainty). Fits are performed using Roberts and Thorne Variable Flavour Number of Scheme to take into accout the heavy quark production.

H1 and ZEUS (prel.)

$Q^2 = 10 \text{ GeV}^2$

April 2010

HERA Inclusive Working Group

HERAPDF1.0
total uncertainty
+low energy data
+low energy data, $Q^2 \geq 5 \text{ GeV}^2$
RT VFN STandard
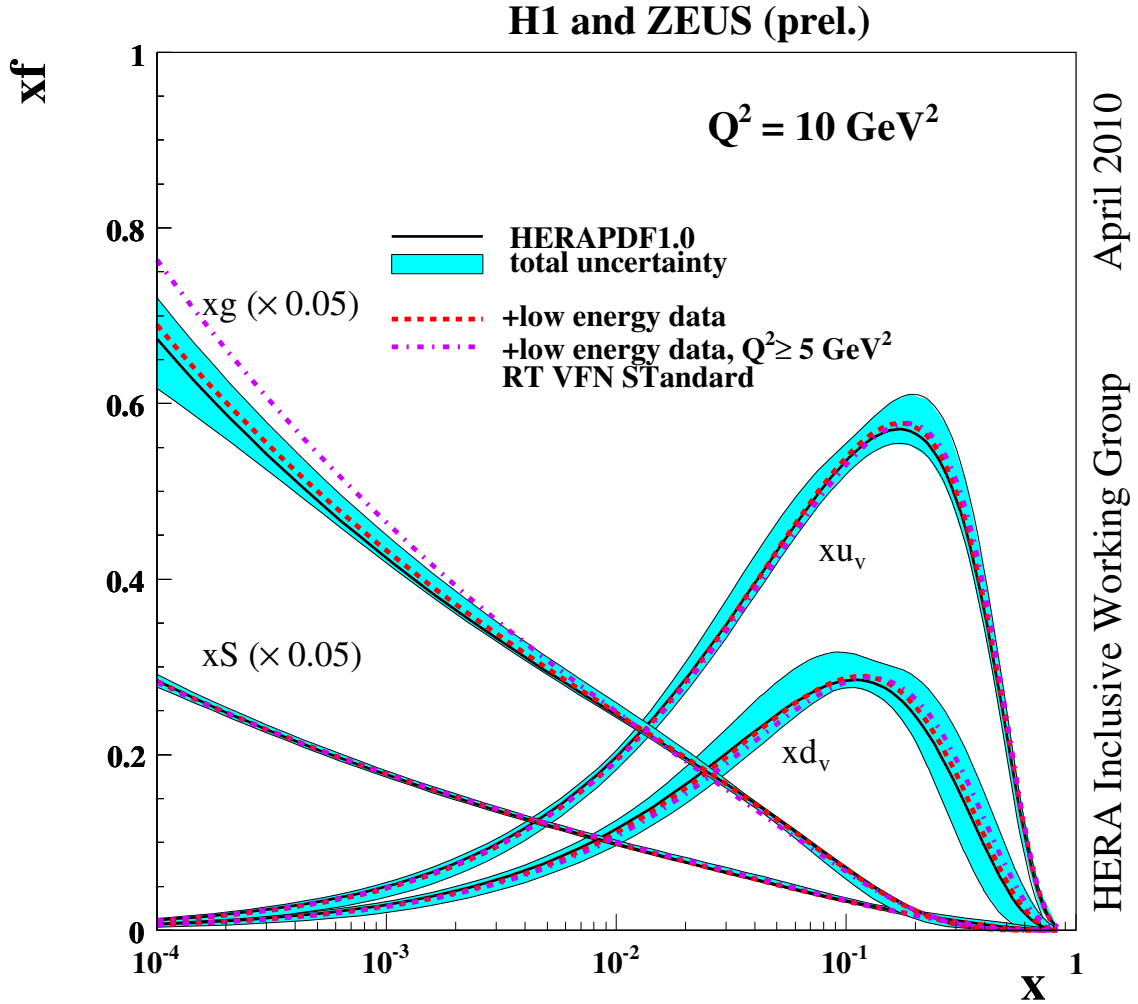
xg ($\times 0.05$)

xS ($\times 0.05$)

xu_v

xd_v

Figure 4: Summary plot of the NLO PDF distributions at the scale $Q_0^2 = 10 \text{ GeV}^2$ shows comparison among HERAPDF1.0 (solid line) with its total PDF uncertainties (blue band), HERA PDF fit with reduced proton-beam energy data using standard settings of HERAPDF1.0 (doted red line) and using $Q^2 > 5 GeV^2$ cut (dashed magenta line). PDF shown are valence distributions for up, down, and distributions for the total sea and gluon. The kinematic cut $Q^2 > 5 GeV^2$ results in a different PDF solution (best visible on the gluon distribution, where the new fit lies outside the HERAPDF1.0 uncertainty). Fits are performed using Roberts and Thorne Variable Flavour Number Scheme to take into accout the heavy quark production.
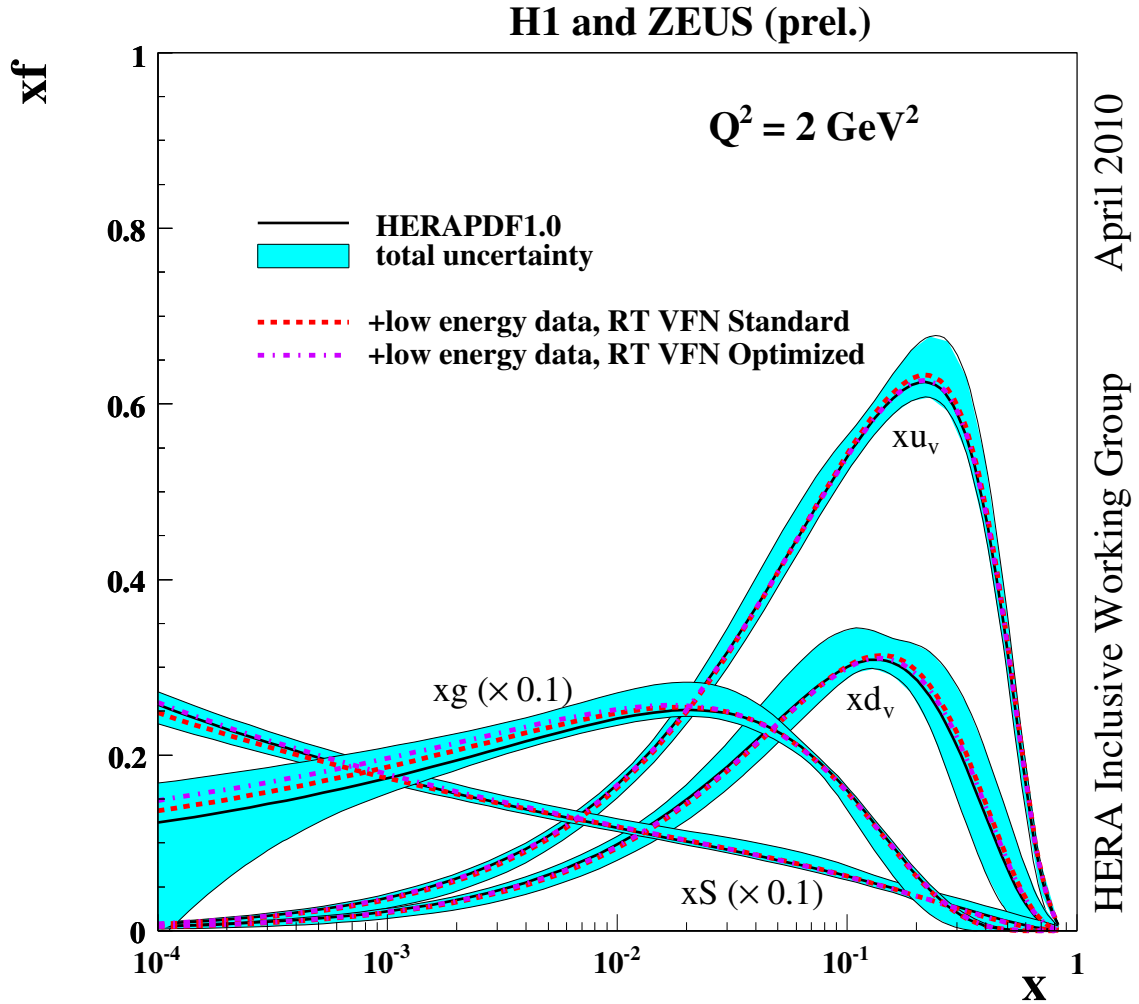
Figure 5: Summary plot of the NLO PDF distributions at the starting scale $Q_0^2 = 1.9$ GeV^2 shows comparison among HERAPDF1.0 (solid line) with its total PDF uncertainties (blue band), HERA PDF fit including reduced proton-beam energy data using standard RT VFN scheme (doted red line) and using optimal RT VFNS scheme (dashed magenta line). PDF shown are valence distributions for up, down, and distributions for the total sea and gluon. The effect of the optimal R VFNS scheme is slightly enhancing the gluon and sea distribution.
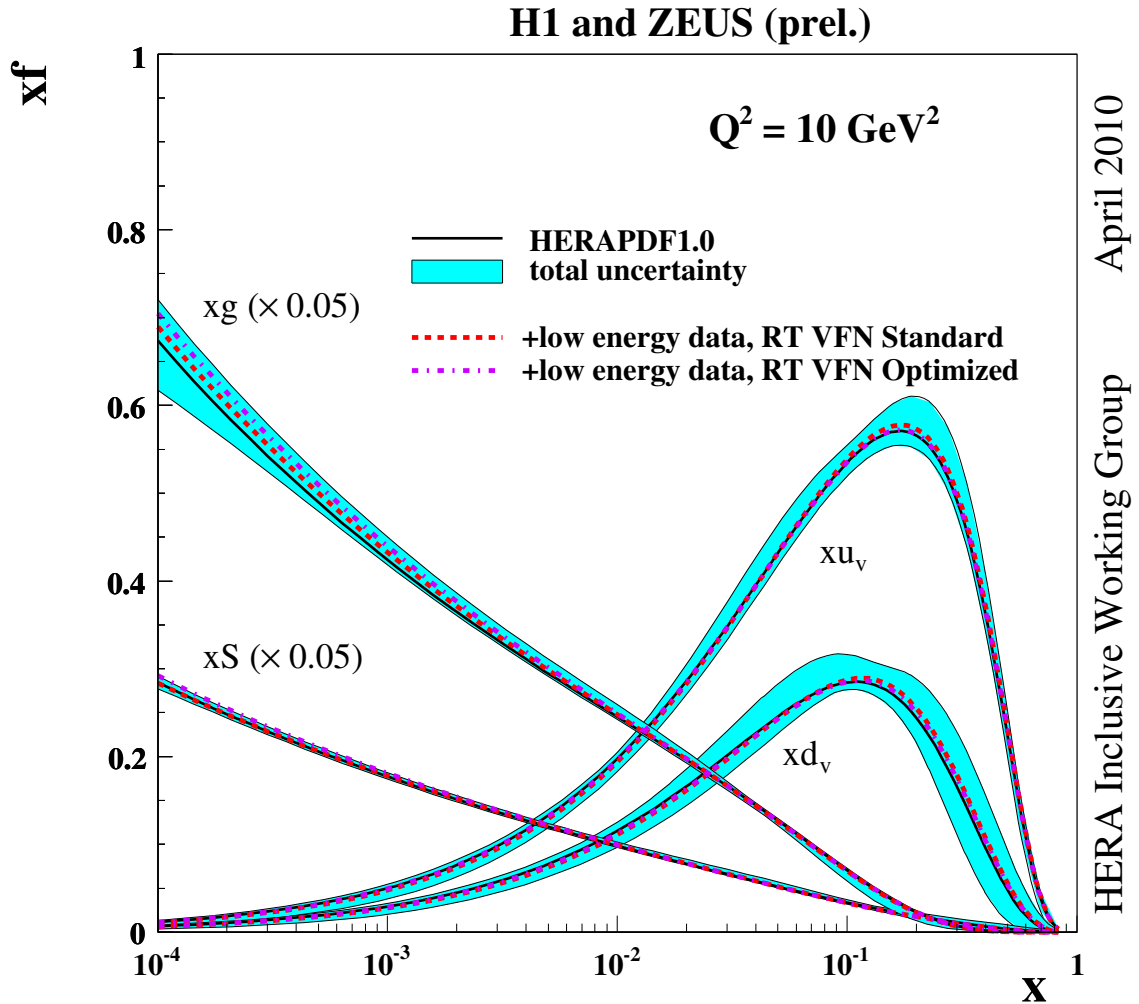
H1 and ZEUS (prel.)

Figure 6: Summary plot of the NLO PDF distributions at the scale $Q_0^2 = 10$ GeV^2 shows comparison among HERAPDF1.0 (solid line) with its total PDF uncertainties (blue band) set, HERA PDF fit including reduced proton-beam energy data using standard RT VFN scheme (doted red line) and using optimal RT VFNS scheme (dashed magenta line). PDF shown are valence distributions for up, down, and distributions for the total sea and gluon. The effect of the optimal R VFNS scheme is slightly enhancing the gluon and sea distribution (effects reduced at this scale).
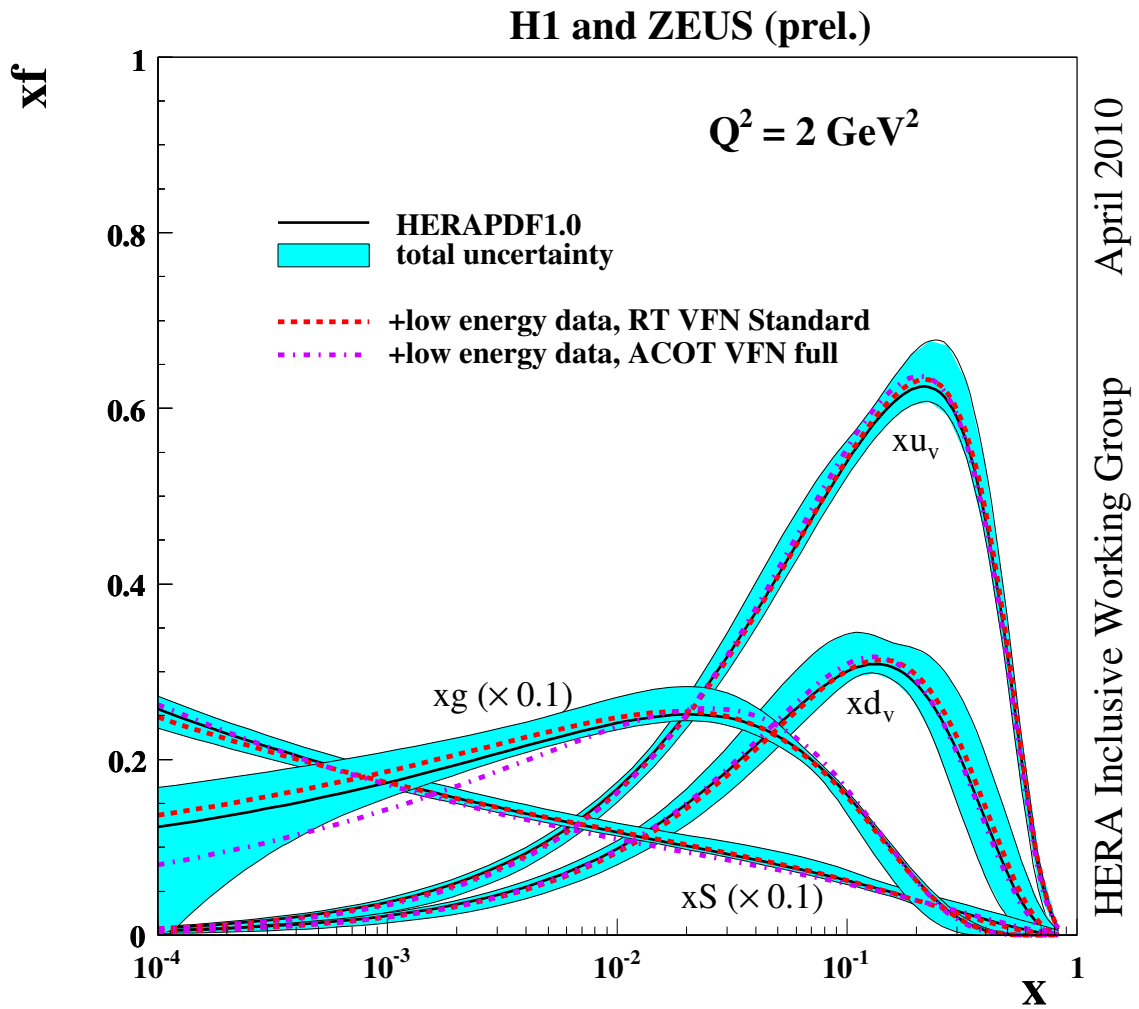
Figure 7: Figure shows the NLO PDF Summary plots at the starting scale of $Q_0^2 = 1.9$ GeV^2 comparing the HERA PDF fits including the low energy runs using RT scheme (red dotted line) to the case of using (full) ACOT scheme (dashed magenta line). HERAPDF1.0 with its error is shown as a refence. The resulting PDFs using ACOT scheme prefer a visibly flatter glon distribution
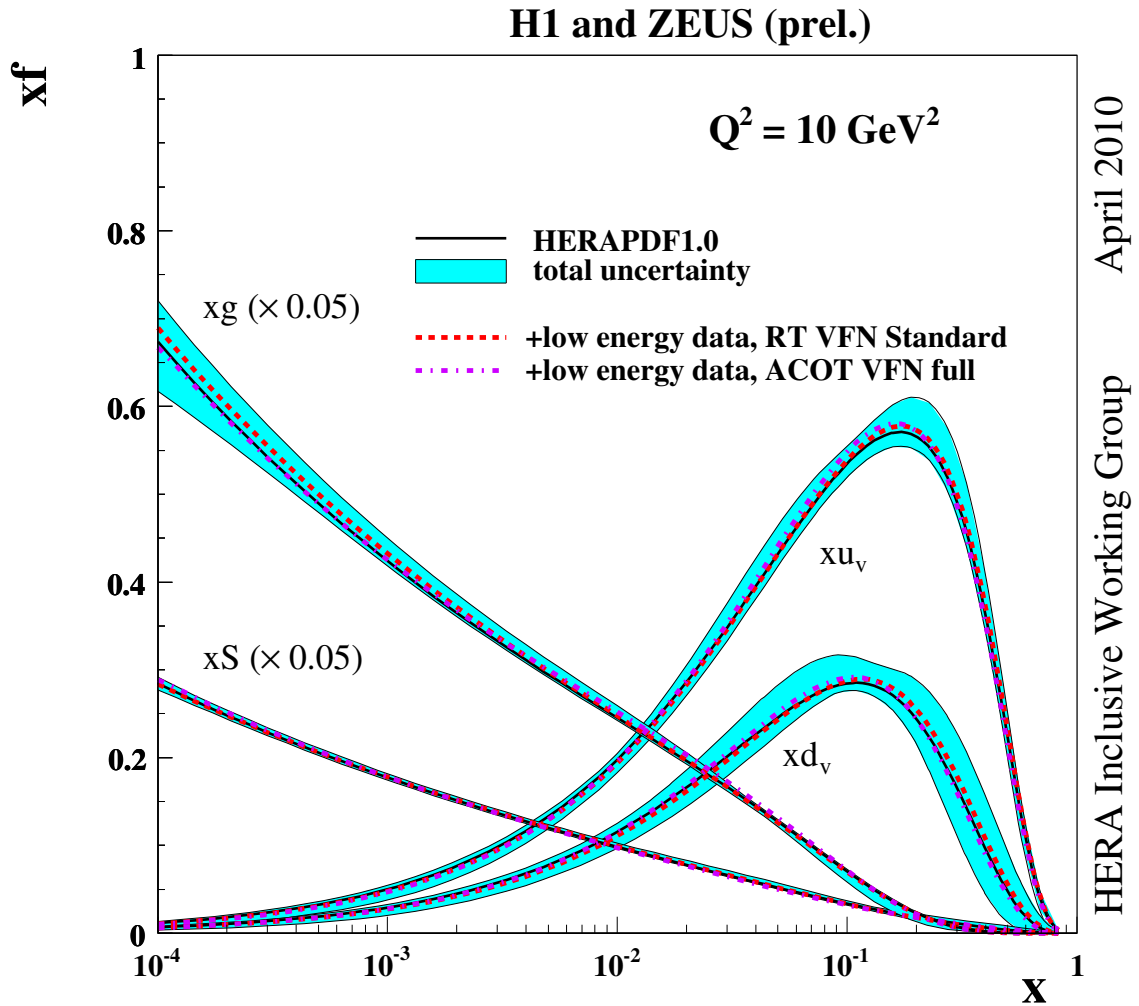
H1 and ZEUS (prel.)

$Q^2 = 10$ GeV^2

April 2010

HERA Inclusive Working Group

HERAPDF1.0
total uncertainty

+low energy data, RT VFN Standard
+low energy data, ACOT VFN full

xg ($\times 0.05$)

xS ($\times 0.05$)

xu$_v$

xd$_v$

Figure 8: Figure shows the NLO PDF Summary plots at the starting scale of $Q_0^2 = 1.9$ GeV^2 comparing the HERA PDF fits including the low energy runs using RT scheme (red dotted line) to the case of using (full) ACOT scheme (dashed magenta line). HERAPDF1.0 with its error is shown as a refence. The resulting PDFs using ACOT scheme prefer a slightly flatter glon distribution, however the differences lie within the uncertainties of HERAPDF1.0 for this scale.
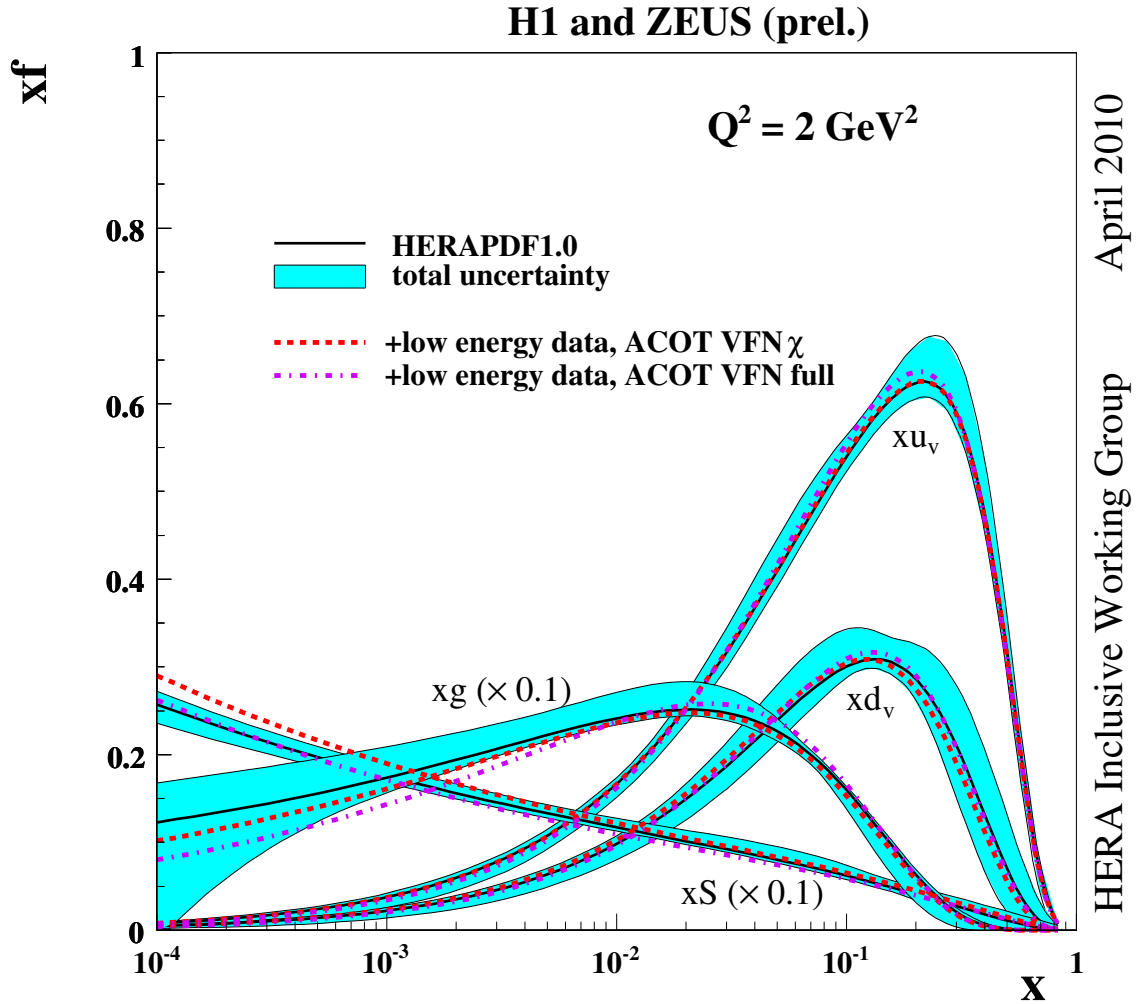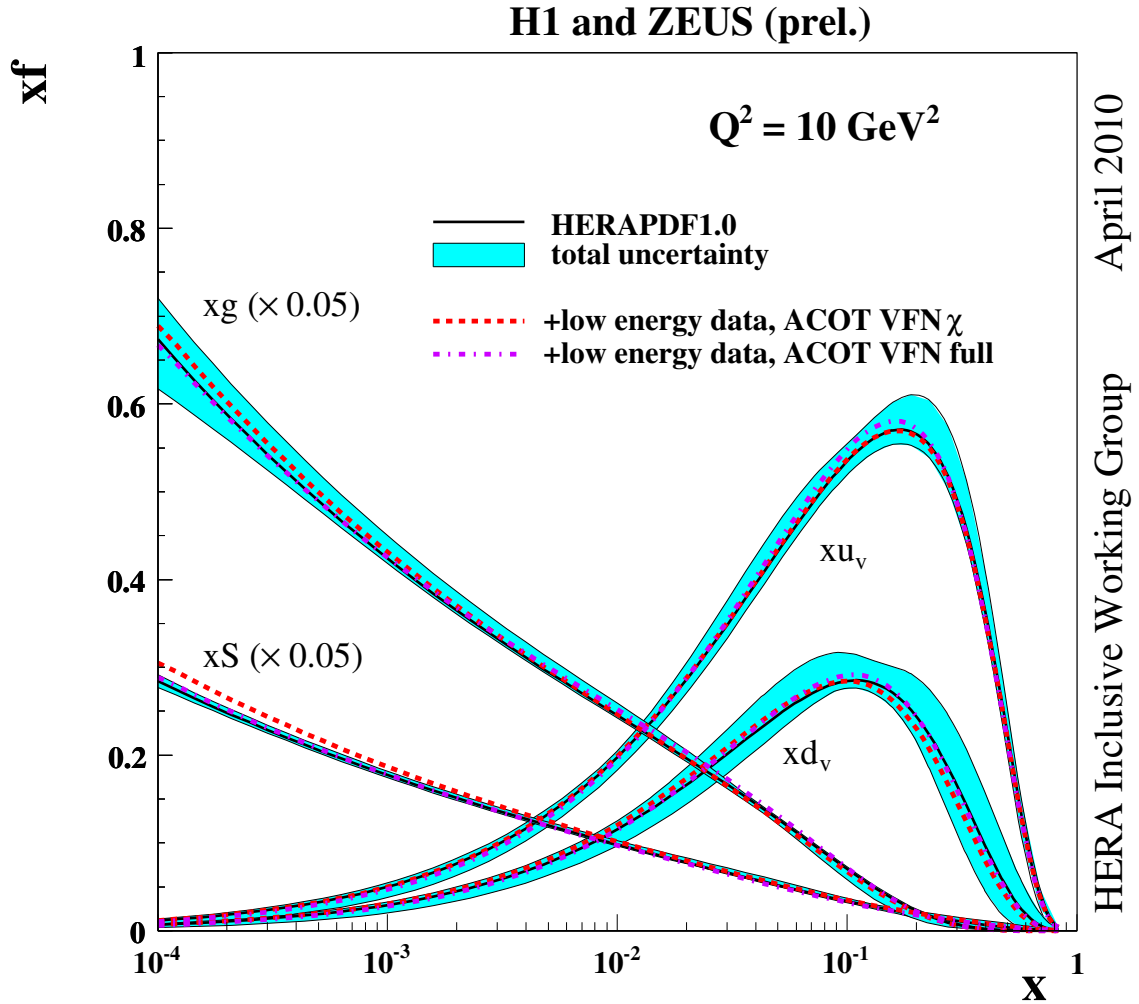
8

Figure 9: Figure shows the NLO PDF Summary plots at the scale of $Q_0^2 = 1.9\,\text{GeV}^2$ comparing the HERA PDF fits including the low energy runs using two variants of the ACOT scheme: χ (red dotted line) and Full (dashed magenta line). The Full ACOT scheme takes all the quark masses into account, the χ scheme provides a smoother transition across the thresholds. HERAPDF1.0 with its error is shown as a refence. The fits using ACOTχ scheme result into a more enhanced gluon and a flatter sea, compared to the full ACOT scheme.

9

Figure 10: Figure shows the NLO PDF Summary plots at the scale of $Q_0^2 = 10\,\text{GeV}^2$ comparing the HERA PDF fits including the low energy runs using two variants of the ACOT scheme: χ (red dotted line) and Full (dashed magenta line). The Full ACOT scheme takes all the quark masses into account, the χ scheme provides a smoother transition across the thresholds. HERAPDF1.0 with its error is shown as a refence. The fits using ACOTχ scheme result into a more enhanced gluon and a flatter sea, compared to the full ACOT scheme.
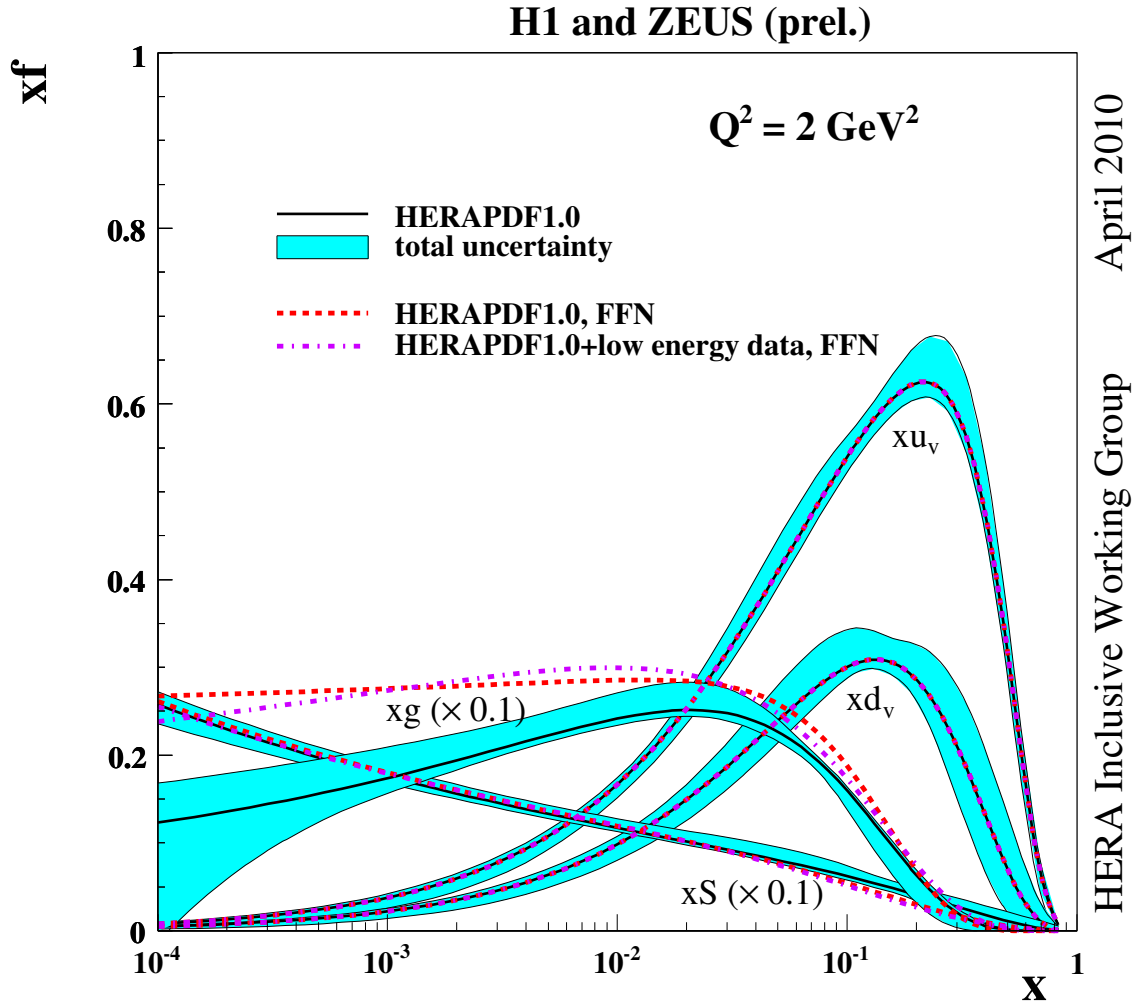
Figure 11: Figure shows the NLO PDF Summary plots at the starting scale of $Q_0^2 = 1.9$ GeV^2 comparing the HERA PDF fits using Fixed Flavour Number Scheme with (red dotted line) and without (dashed magenta line) inclusion of the the low energy runs using FFNS scheme. HERAPDF1.0 with its error is shown as a refence. Differences are due to different schemes. PDFs in FFNS scheme were produced using $\alpha_S(M_Z) = 0.103$ at $n_f = 3$. Inclusion of the low energy data brings little effect on the quality of the fit and PDF shapes.
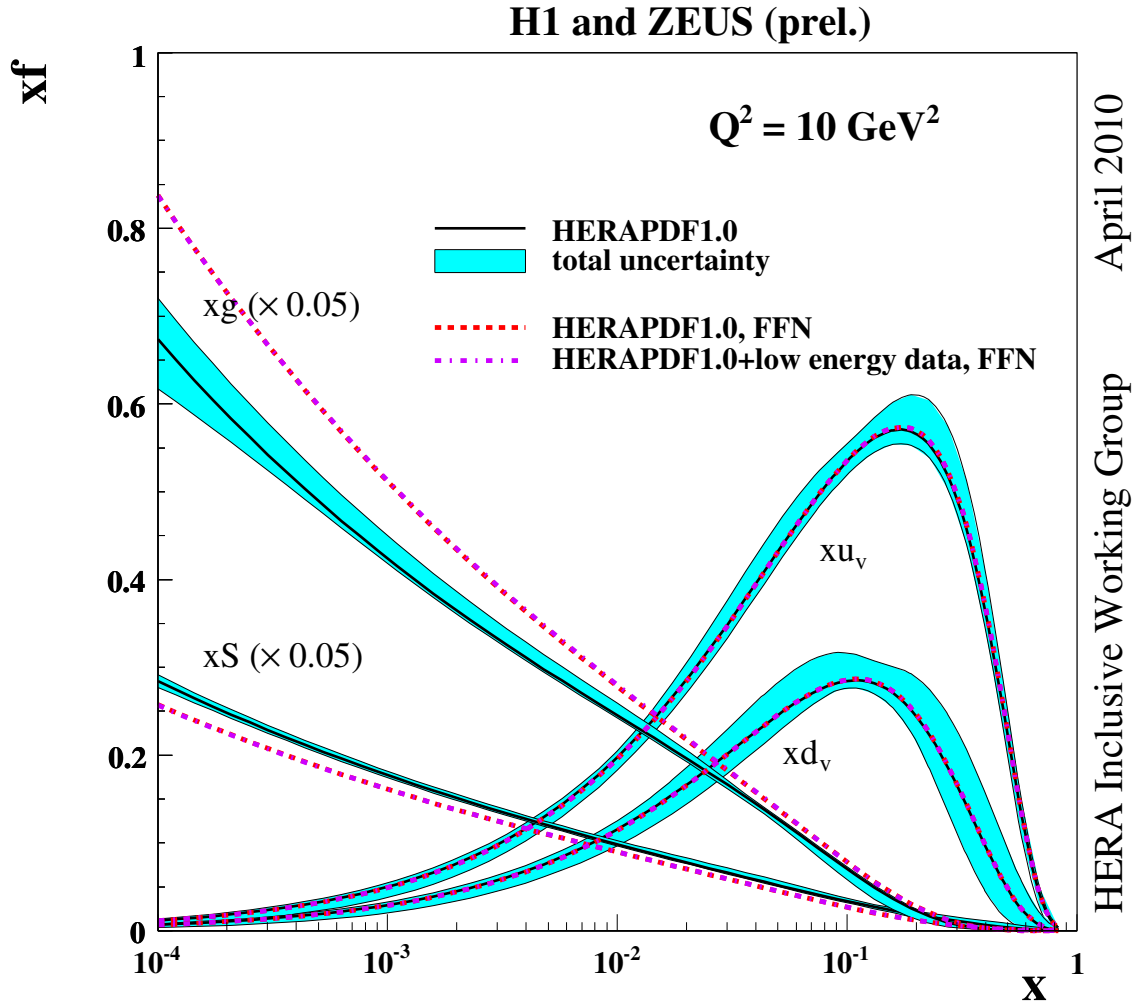
Figure 12: Figure shows the NLO PDF Summary plots at the scale of $Q_0^2 = 10$ GeV^2 comparing the HERA PDF fits using Fixed Flavour Number Scheme with (red dotted line) and without (dashed magenta line) inclusion of the the low energy runs using FFNS scheme. HERAPDF1.0 with its error is shown as a refence. Differences are due to different schemes. PDFs in FFNS scheme were produced using $\alpha_S(M_Z) = 0.103$ at $n_f = 3$. Inclusion of the low energy data brings little effect on the quality of the fit and PDF shapes.
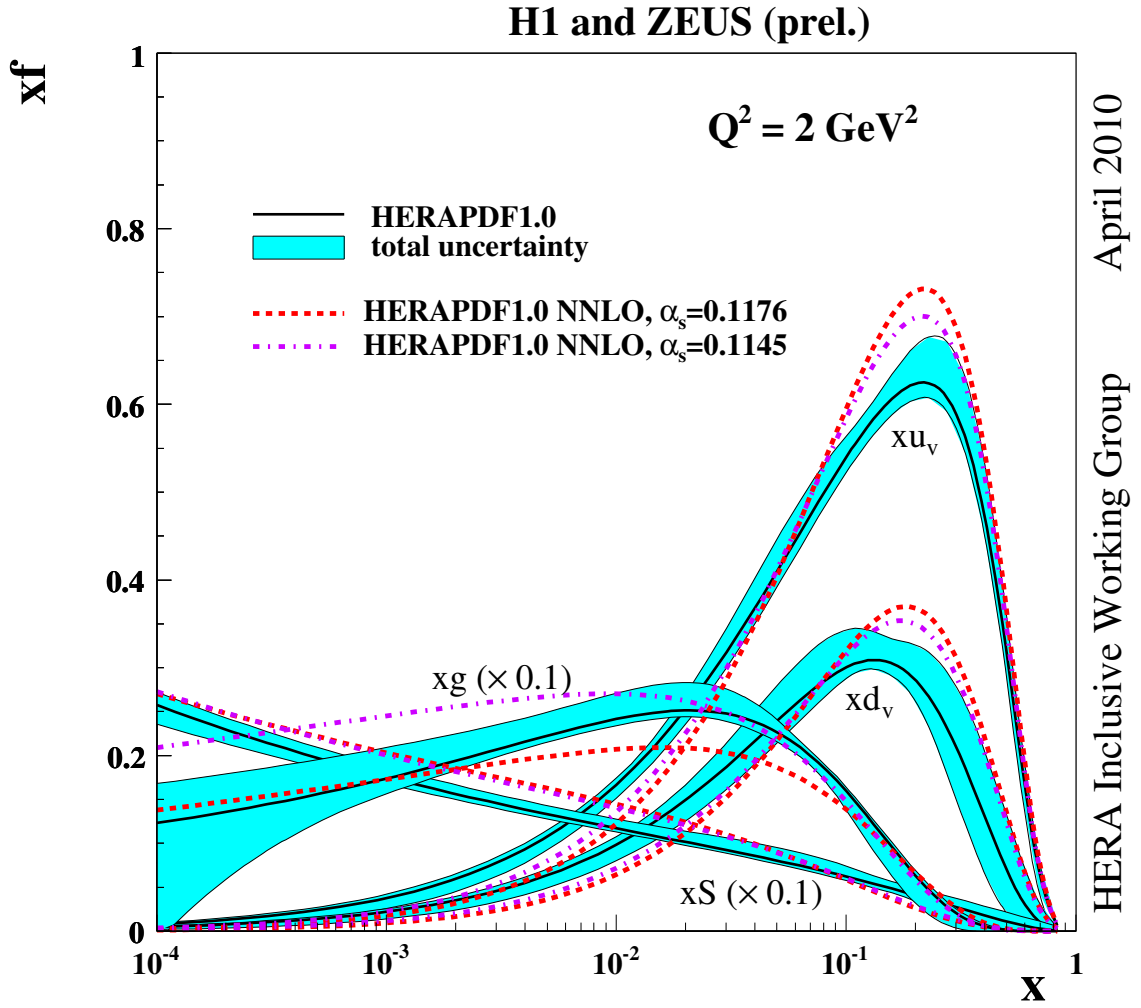
Figure 13: Figure shows the PDF Summary plots at the starting scale of $Q_0^2 = 1.9$ GeV^2 comparing the NNLO HERA PDF fits for different $\alpha_S(M_Z)$: at 0.1176 (red dotted line) and at 0.1145 (magenta dashed line) using the same data sets and other settings as for the HERAPDF1.0. HERAPDF1.0 with its error is shown as a refence. All plots were produced using RT VFNS. The NNLO distributions are different from NLO.

$\alpha_S(M_Z)$	NNLO fits	without low energy data	with low energy data
0.1176	$\Delta\chi^2$	64	75
0.1145	$\Delta\chi^2$	49	55

Table 2: Differences in the total chisquare between NLO and NNLO fits using same settings as for HERAPDF1.0, with and without low energy data runs. The diffeerences in units of χ^2 are shown for two values of the strong coupling. NNLO fits result in a worse quality of the agreement regardless of the inclusion of new data. The NNLO fits were performed using RT VFN scheme.
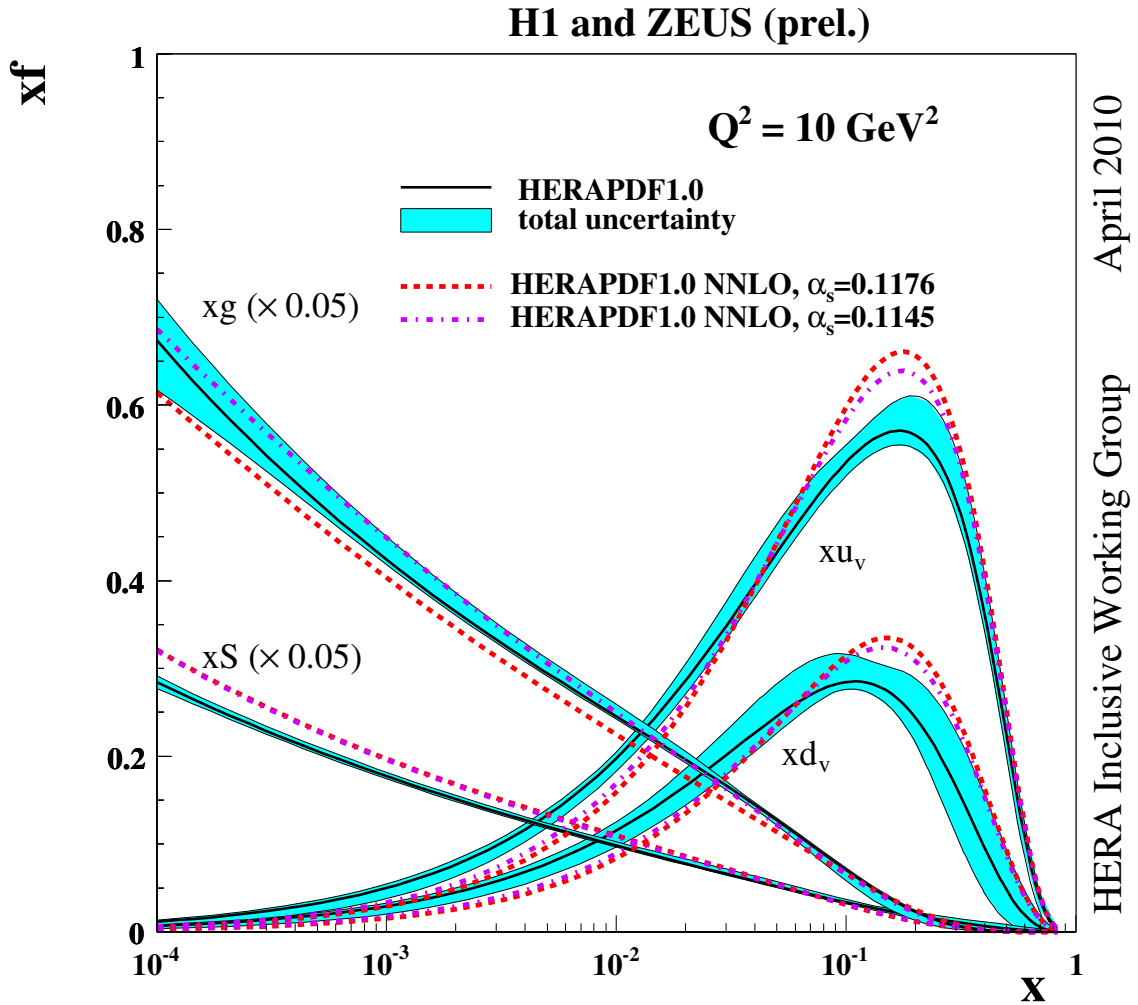
Figure 14: Figure shows the PDF Summary plots at the scale of $Q_0^2 = 10$ GeV^2 comparing the NNLO HERA PDF fits for different $\alpha_S(M_Z)$: at 0.1176 (red dotted line) and at 0.1145 (magenta dashed line) using the same data sets and other settings as for the HERAPDF1.0. HERAPDF1.0 with its error is shown as a refence. All plots were produced using RT VFNS. The NNLO distributions are different from NLO.

HERA I + Reduced Proton-Beam Eneregy Data	Standard Settings	$Q^2 \geq 5$ GeV^2
Total χ^2/dof	818/806	698/771

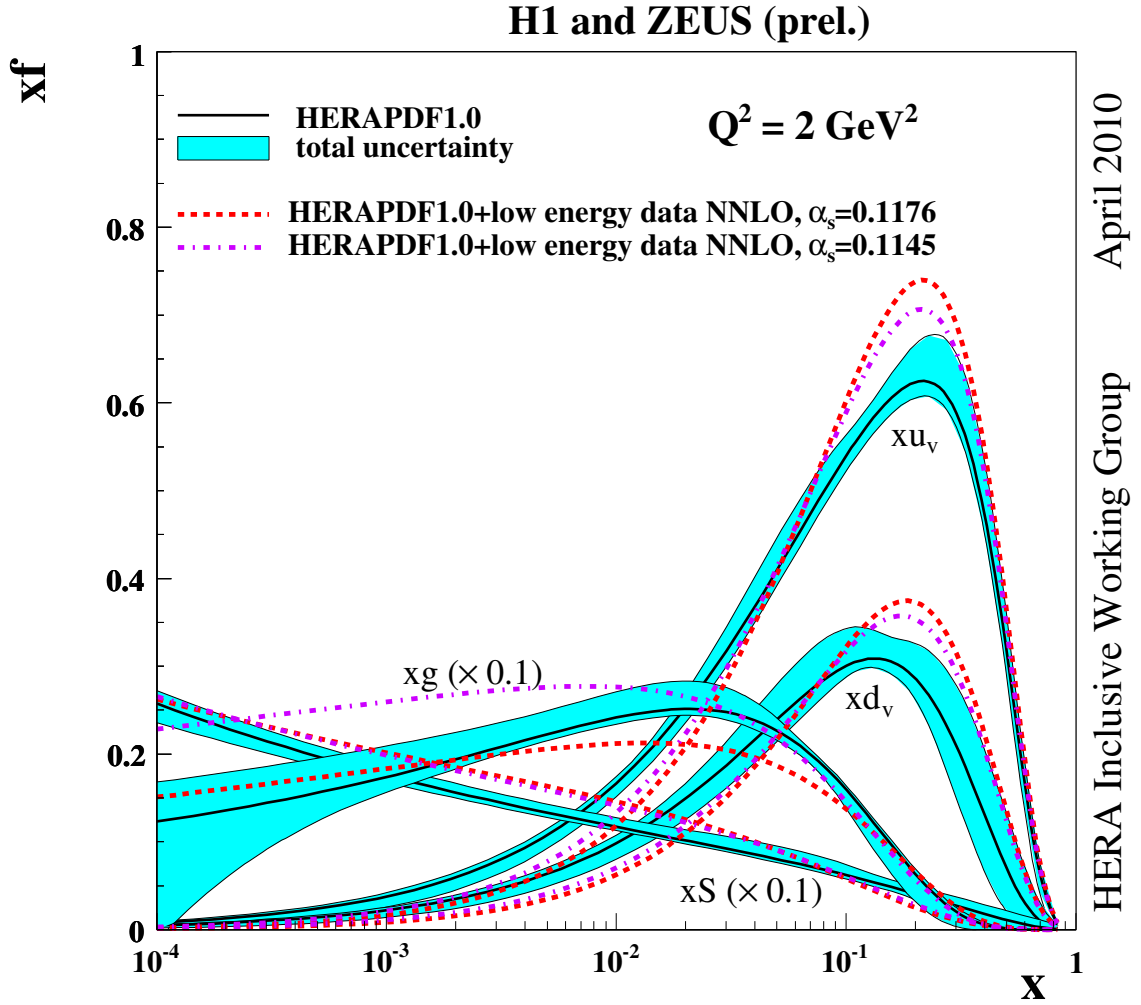Table 3: Comparison of the goodness of the fit between HERAPDF1.0 and adding the low energy data.

Figure 15: Figure shows the PDF Summary plots at the starting scale of $Q_0^2 = 1.9$ GeV^2 comparing the NNLO HERA PDF fits produced at different $\alpha_S(M_Z)$: at 0.1176 (red dotted line) and at 0.1145 (magenta dashed line) including the low energy data run. HERAPDF1.0 with its error is shown as a refence. All plots were produced using RT VFNS. The NNLO distributions are different from NLO with gluon evolution slower and sea faster. No significant effect is observed after inclusion of low energy data.

	RT standard	RT optimal	ACOT full	ACOTχ
$\Delta\chi^2$	0	7	30	25

Table 4: Differences in the total chisquare with respect to the standard settings for fits which include HERA low energy runs, for which $\chi^2 = 818$
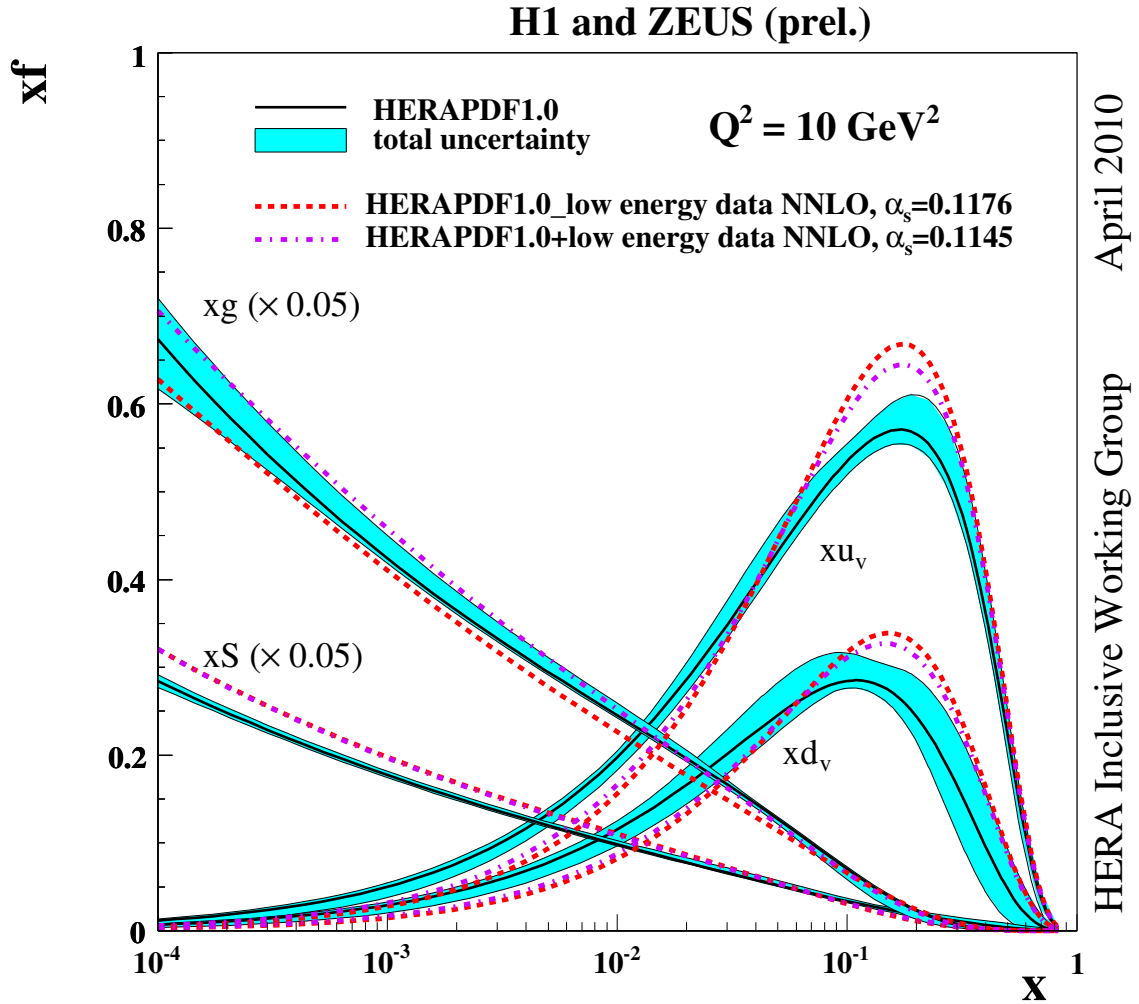
Figure 16: Figure shows the PDF Summary plots at the scale of $Q_0^2 = 10 \text{ GeV}^2$ comparing the NNLO HERA PDF fits produced at different $\alpha_S(M_Z)$: at 0.1176 (red dotted line) and at 0.1145 (magenta dashed line) including the low energy data run. HERAPDF1.0 with its error is shown as a refence. All plots were produced using RT VFNS. The NNLO distributions are different from NLO with gluon evolution slower and sea faster. No significant effect is observed after inclusion of low energy data.
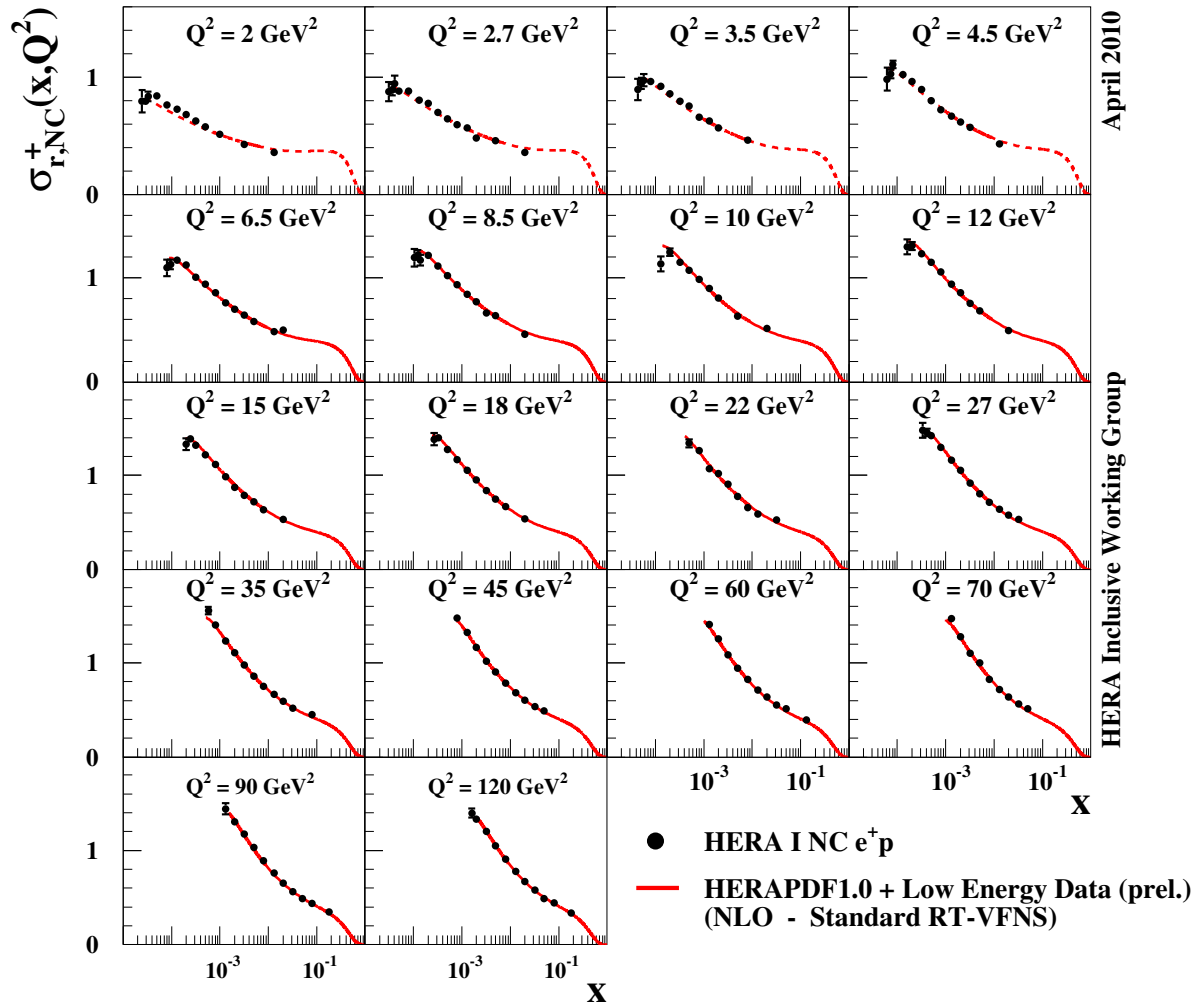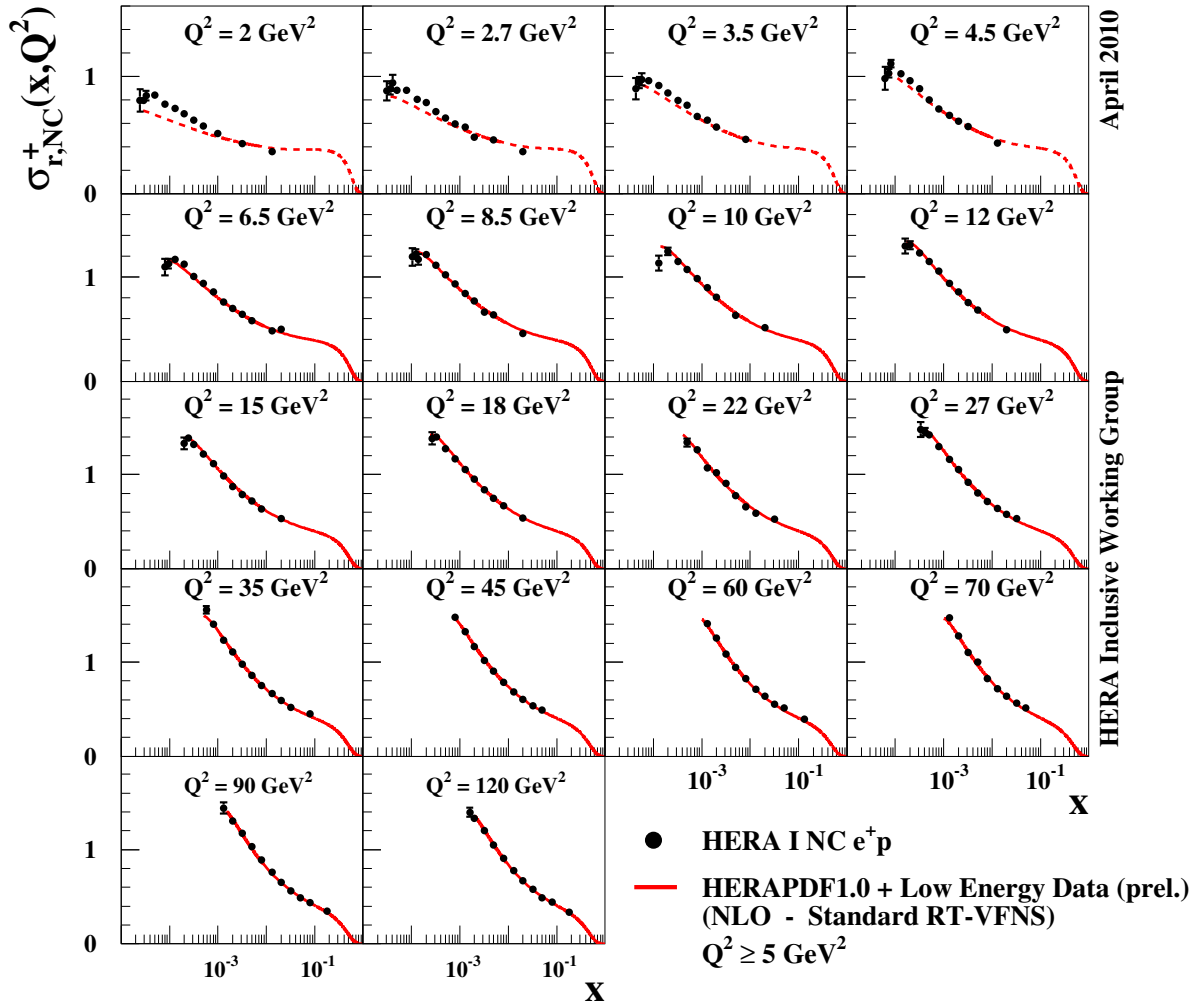
Figure 17: Figure shows the NC cross section data of 920 GeV proton beam as function of x for all Q^2 bins with HERAPDF fit (red line). Fit is produced using standard HERAPDF1.0 settings including low energy data ($Q^2 \geq 3.5$ GeV^2 cut). Fit describes well data, even the lowest Q^2 bins which are not included in the fit. Very little turn over is observed for 920 GeV data.

Figure 18: Figure shows the NC cross section data of 920 GeV proton beam as function of x for all Q^2 bins with HERAPDF fit (red line). Fit is produced using standard HERAPDF1.0 settings, but with $Q^2 \geq 5\,\text{GeV}^2$ cut, including low energy data. Bad description in the region where data does not enter in the fit.
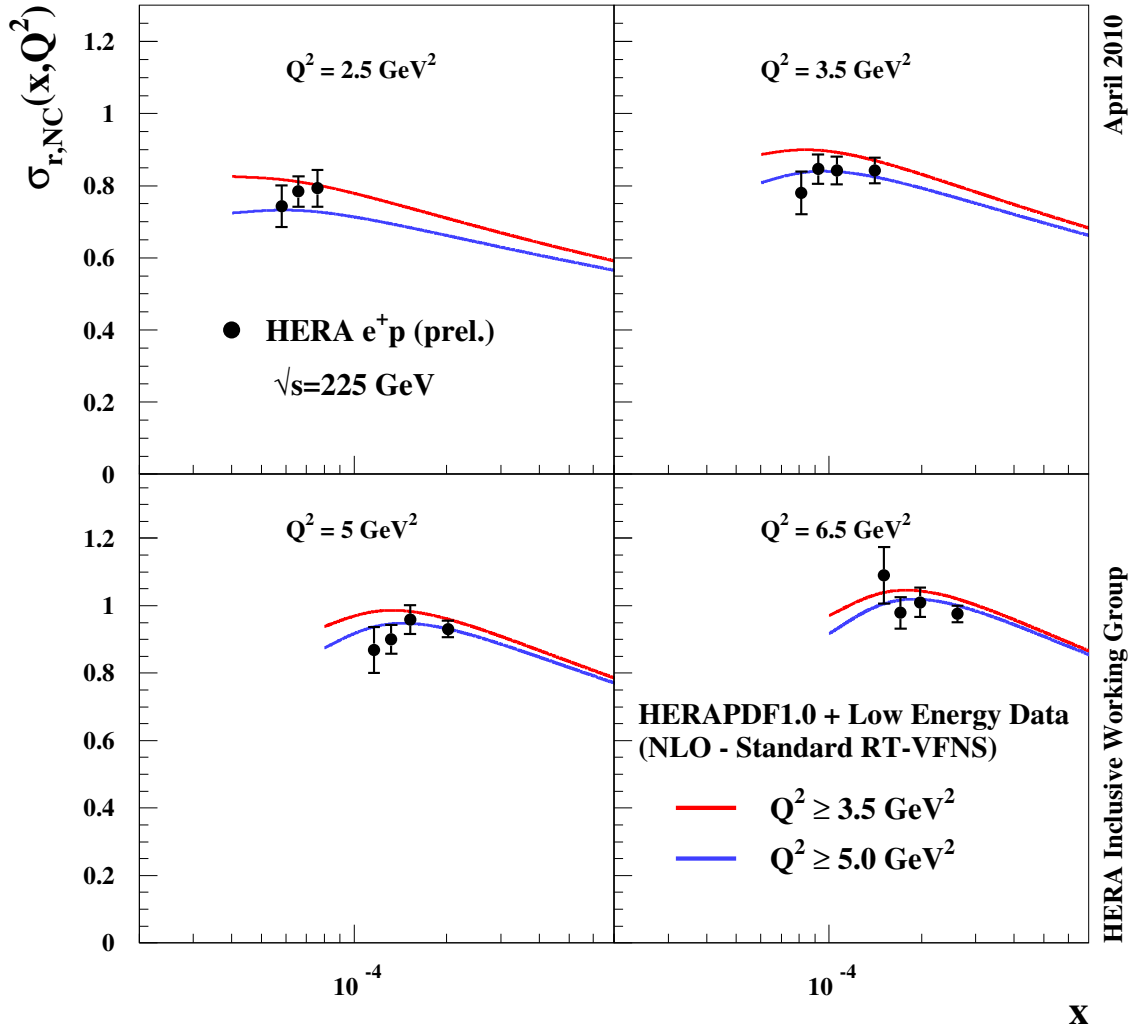
Figure 19: Figure shows the NC cross section data of 460 GeV proton beam as function of x for low Q^2 bins with HERAPDF fit (red line). Fit is produced using standard HERAPDF1.0 settings, with $Q^2 \geq 5\ GeV^2$ cut (blue), and $Q^2 \geq 3.5\ GeV^2$ cut (red), including low energy data with. The Q^2 cut fits better the 460 GeV data.
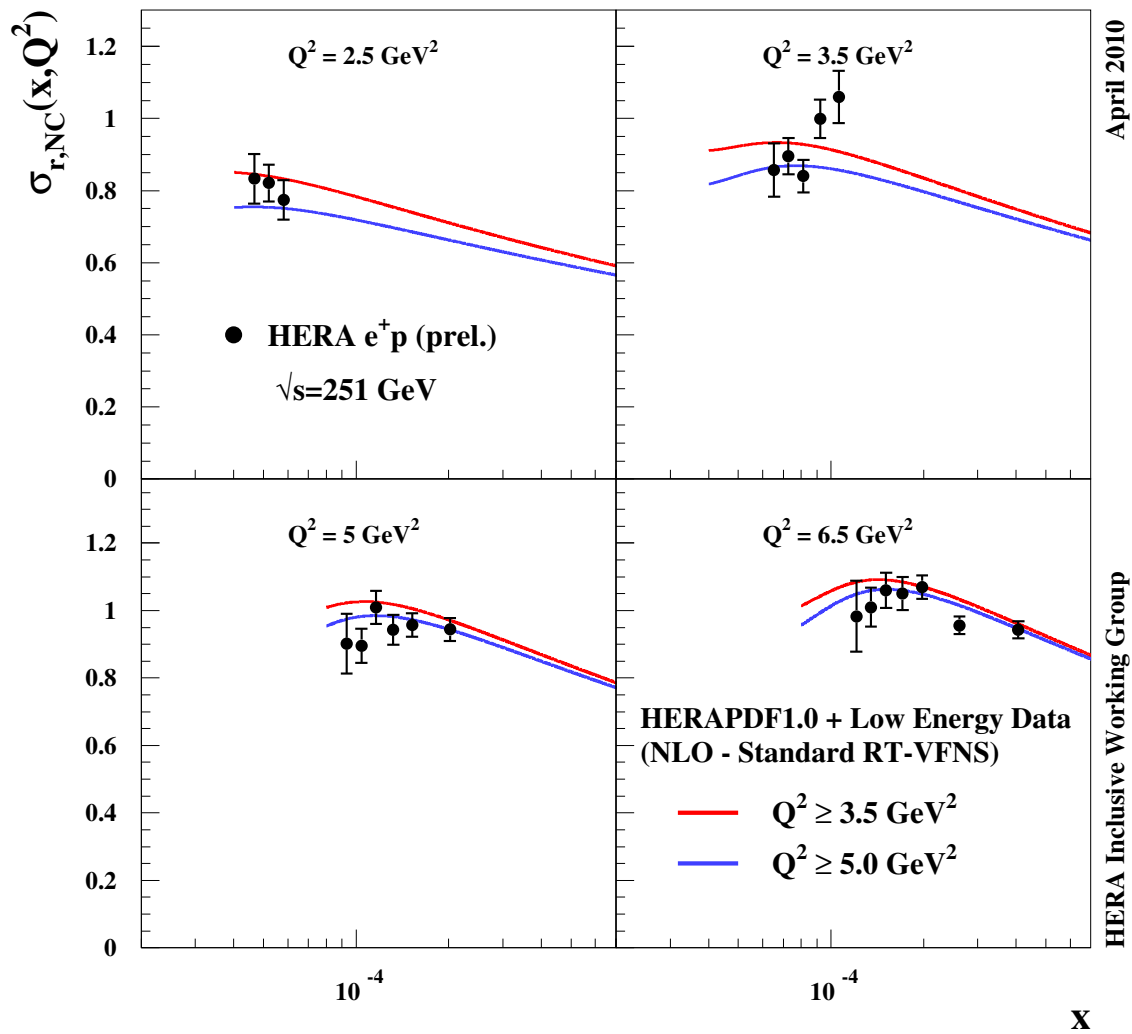
H1 and ZEUS

Figure 20: Figure shows the NC cross section data of 575 GeV proton beam as function of x for low Q^2 bins with HERAPDF fit (red line). Fit is produced using standard HERAPDF1.0 settings, with $Q^2 \geq 5\ GeV^2$ cut (blue), and $Q^2 \geq 3.5\ GeV^2$ cut (red), including low energy data with.
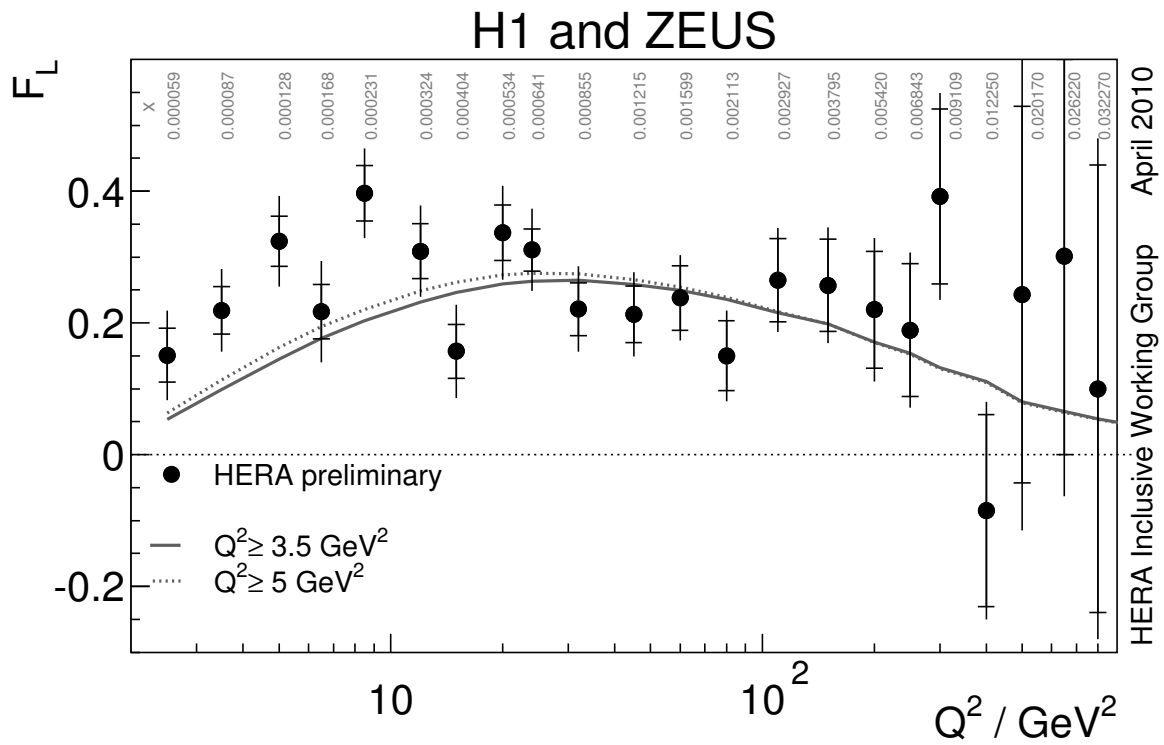
Figure 21: Figure shows the Combined H1 and ZEUS F_L data as function of the Q^2 averaged in x bins versus predictions from HERAPDF fits which includes the low energy data runs with the $Q^2 \geq 5$ GeV^2 cut and without. HERAPDF1.0 is also shown as a reference. The variation of the cut has very little effect.
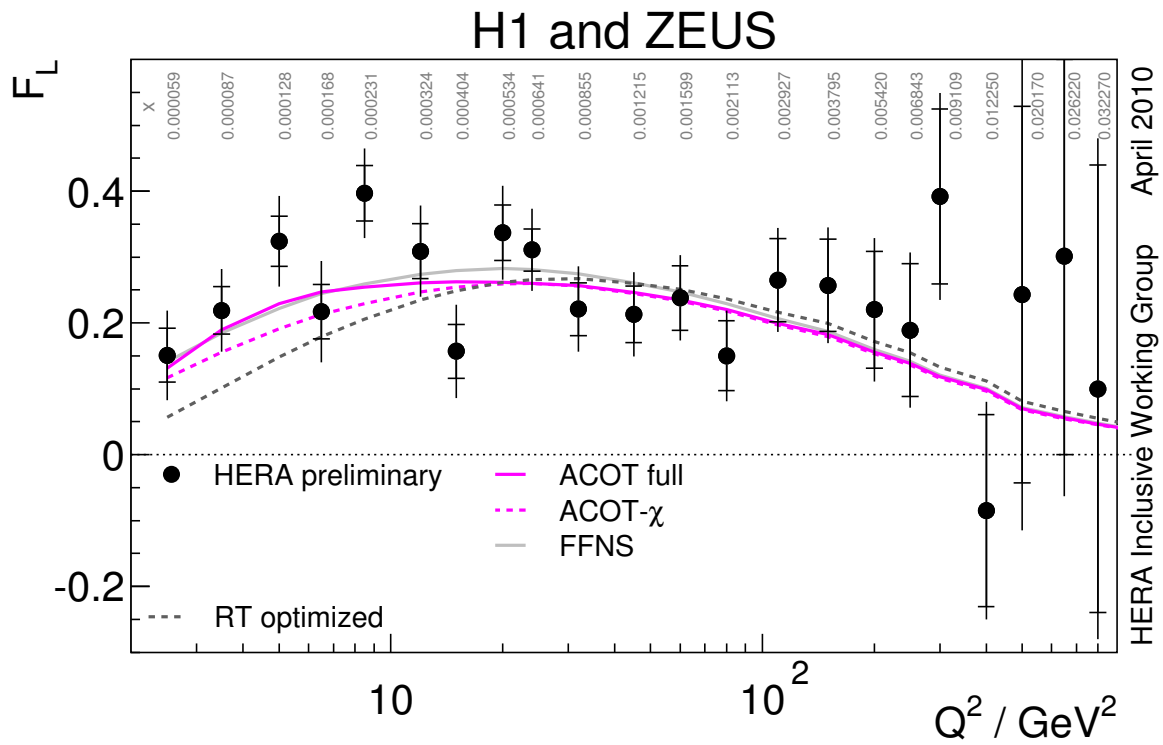
Figure 22: Figure shows the Combined H1 and ZEUS F_L data as function of the Q^2 averaged in x bins versus predictions from HERAPDF fits performed under various heavy flavour treatments: ACOT (χ and Full), RT (standard and optimal), FFNS. Interesting to observe that ACOT and FFN return a better prediction for the F_L data.
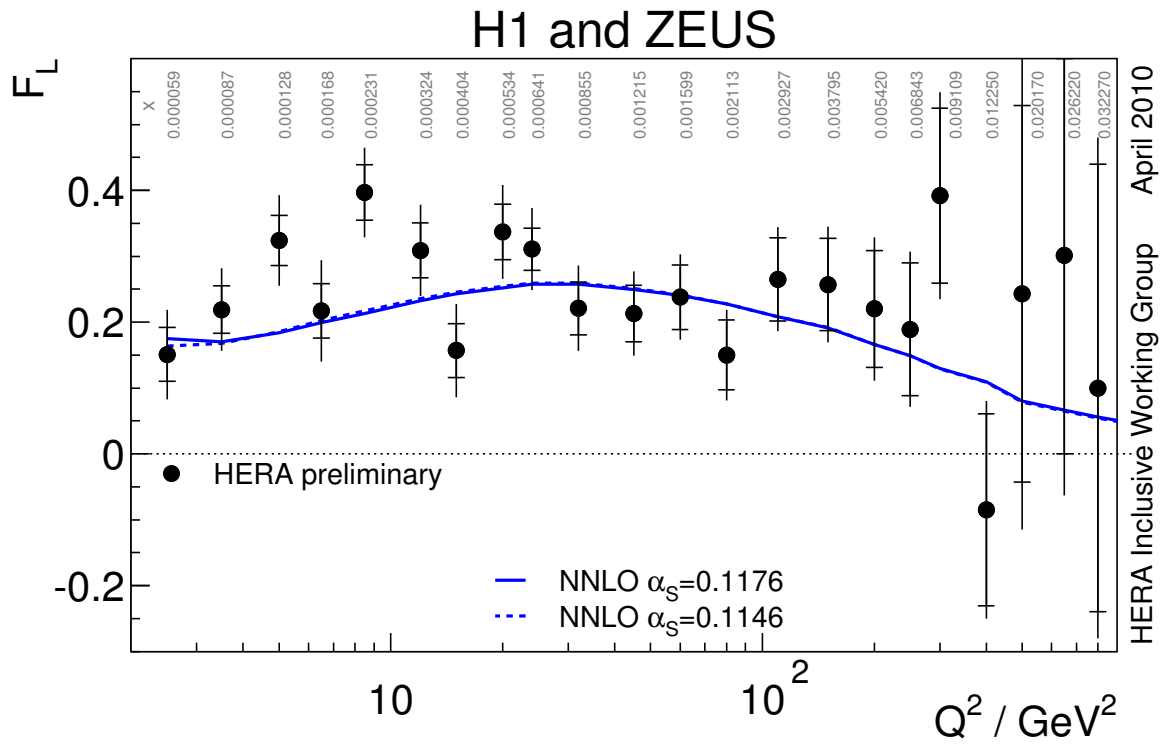
Figure 23: Figure shows the Combined H1 and ZEUS F_L data as function of the Q^2 averaged in x bins versus predictions from HERAPDF fits at NNLO for two different α_S values (0.1145 and 0.1176). The predictions at NNLO seem to return in a better description of the F_L data.